PHILOSOPHICAL TRANSACTIONS B

royalsocietypublishing.org/journal/rstb

Research

Cite this article: Himmel NJ, Letcher JM, Sakurai A, Gray TR, Benson MN, Cox DN. 2019 *Drosophila* menthol sensitivity and the Precambrian origins of transient receptor potential-dependent chemosensation. *Phil. Trans. R. Soc. B* **374**: 20190369.
http://dx.doi.org/10.1098/rstb.2019.0369

Accepted: 9 July 2019

One contribution of 19 to a Theo Murphy meeting issue 'Evolution of mechanisms and behaviour important for pain'.

Subject Areas:
neuroscience

Keywords:
TRP channels, *Drosophila*, nociception, menthol, chemosensation, evolution

Authors for correspondence:
Nathaniel J. Himmel
e-mail: nhimmel1@student.gsu.edu
Daniel N. Cox
e-mail: dcox18@gsu.edu

Electronic supplementary material is available online at https://dx.doi.org/10.6084/m9.figshare.c.4614923.

THE ROYAL SOCIETY PUBLISHING

Drosophila menthol sensitivity and the Precambrian origins of transient receptor potential-dependent chemosensation

Nathaniel J. Himmel, Jamin M. Letcher, Akira Sakurai, Thomas R. Gray, Maggie N. Benson and Daniel N. Cox

Neuroscience Institute, Georgia State University, Atlanta, GA 30302, USA

NJH, 0000-0001-7876-6960; JML, 0000-0003-3077-0615; AS, 0000-0003-2858-1620; TRG, 0000-0002-6176-005X; DNC, 0000-0001-9191-9212

Transient receptor potential (TRP) cation channels are highly conserved, polymodal sensors which respond to a wide variety of stimuli. Perhaps most notably, TRP channels serve critical functions in nociception and pain. A growing body of evidence suggests that transient receptor potential melastatin (TRPM) and transient receptor potential ankyrin (TRPA) thermal and electrophile sensitivities predate the protostome–deuterostome split (greater than 550 Ma). However, TRPM and TRPA channels are also thought to detect modified terpenes (e.g. menthol). Although terpenoids like menthol are thought to be aversive and/or harmful to insects, mechanistic sensitivity studies have been largely restricted to chordates. Furthermore, it is unknown if TRP-menthol sensing is as ancient as thermal and/or electrophile sensitivity. Combining genetic, optical, electrophysiological, behavioural and phylogenetic approaches, we tested the hypothesis that insect TRP channels play a conserved role in menthol sensing. We found that topical application of menthol to *Drosophila melanogaster* larvae elicits a *Trpm*- and *TrpA1*-dependent nocifensive rolling behaviour, which requires activation of Class IV nociceptor neurons. Further, in characterizing the evolution of TRP channels, we put forth the hypotheses that three previously undescribed TRPM channel clades (basal, αTRPM and βTRPM), as well as TRPs with residues critical for menthol sensing, were present in ancestral bilaterians.

This article is part of the Theo Murphy meeting issue 'Evolution of mechanisms and behaviour important for pain'.

1. Introduction

Menthol and icilin are often referred to as 'cooling agents'—while these chemicals do not physically chill, topical application typically elicits a pleasant cooling sensation in humans [1]. Perhaps owing to its perceived cooling properties, menthol has been used as a topical analgesic, often to reduce the severity of itching and/or burning sensations [2–4]. That said, what is pleasant, harmful, or potentially painful will often be species-dependent. It has been previously reported that menthol affects the behaviour of insects; for example, menthol-infused foods are aversive to *Drosophila melanogaster*, and there is some evidence that menthol functions as an insecticide [5–11]. However, relatively little is known concerning the mechanisms by which insects sense and respond to the cooling agents, as previous studies have focused largely on deuterostomes, and, with respect to molecular determinants among those species, chiefly on terrestrial chordates [12–20]. By extension, it is unknown if possible shared mechanisms have their origins in a common ancestor.

Like many other compounds, menthol and icilin are thought to be detected by transient receptor potential (TRP) channels—primarily transient receptor potential melastatin (TRPM)8 and transient receptor potential ankyrin (TRPA)1 [17,21,22]. TRP channels are variably selective cation channels which are differentially gated by a wide variety of thermal, chemical and mechanical stimuli. It is the multimodal nature of TRPM8 and TRPA1—in humans constituted by at

least menthol, icilin, and cold sensing—which partly underlies the similar phenomenological character (i.e. cooling) associated with these very different stimuli [22–24].

The chordate TRPM family is typically divided into eight distinct paralogues (TRPM1-TRPM8) thought to have emerged sometime prior to the divergence of tetrapods and fishes (although fishes are thought to have lost their TRPM8 orthologue) [25]. TRPM8 is multimodal, responding to cold, menthol, and in mammals, icilin [22,26]. It has been suggested that menthol directly binds with the TRPM8 voltage sensor-like domain (VSLD), and gating requires interactions between this domain, bound menthol molecules, and the highly conserved C-terminal TRP domain [13,20]. TRPM8-menthol gating has been well characterized in mammalian channels, and a number of critical amino acid residues have been identified in both the VSLD and the TRP domain [12,14,16,19,20].

In contrast to the TRPM family, the chordate TRPA family is very small, typically containing only a single member, TRPA1 [27,28]. TRPA1 is a polymodal nociceptor involved in the detection of noxious cold, noxious heat, menthol, icilin and electrophilic chemicals such as allyl isothiocyanate (AITC, found in mustard oil and wasabi) [21,24,29,30]. It has been suggested that TRPA1 menthol sensitivity is linked to specific serine and threonine residues found in transmembrane segment 5, and that several nearby residues are responsible for species-specific TRPA1-menthol interactions [31].

Insects lack a true TRPM8 orthologue. In fact, the *Drosophila* genome contains only a single TRPM family gene, *Trpm* (figure 1, top) [32]. While separated by several gene duplication events and more than 550 million years of evolution, *Drosophila* Trpm and its chordate counterpart, TRPM8, are both involved in cold sensing [33]. With respect to TRPAs, the *Drosophila* genome encodes four TRPA family genes (figure 1, bottom): *TrpA1* (the homologue to chordate *TRPA1*), *painless* (*pain*), *water witch* (*wtrw*), and *pyrexia* (*pyx*). Like vertebrate TRPA1, *Drosophila* TrpA1 has been implicated in high-temperature and chemical nociception [27,33–37].

TRPA1 high-temperature and electrophile sensitivities are present in both protostomes and deuterostomes [27,36–45]. While current evidence suggests—despite some controversy—that TRPA1 cold sensitivity evolved relatively recently, perhaps among early synapsids (less than 300 Ma) [46–48], TRPM cold sensitivity is conserved in insects [33]. As such, a growing body of evidence suggests that TRP channel thermal and electrophile sensitivity may have a common origin predating the protostome–deuterostome split (greater than 550 Ma). However, it remains unknown if TRPA- and TRPM-dependent menthol sensitivity is equally ancient.

In order to further elucidate the evolutionary history of TRPM and TRPA channels, we explored the mechanisms by which *Drosophila* senses and responds to cooling agents. Herein, we report that topical menthol application elicits a dose-dependent nocifensive rolling behaviour in *Drosophila*. Further, we use a suite of genetic, optical, electrophysiological and behavioural approaches to demonstrate that the menthol-evoked response is *Trpm*- and *TrpA1*-dependent, and acts via Class IV (CIV) nociceptors. Finally, in light of these findings, we assess the evolutionary histories and sequence homologies of TRPM and TRPA channels. In doing so, we characterize several putative TRPM and TRPA channels in *Acropora digitifera* (coral), *Strongylocentrotus purpuratus* (purple sea urchin), *Octopus bimaculoides* (California two-spot octopus), *Priapulus caudatus* (penis worm) and *Aplysia californica* (California sea hare), as well as outline the discovery of three previously undescribed TRPM channel clades (basal TRPMs, αTRPMs and βTRPMs), which we hypothesize were present in the last common bilaterian ancestor, Urbilateria. The results of these studies add to a growing body of evidence suggesting that chemosensation and nociception have functional origins in the Precambrian world [49].

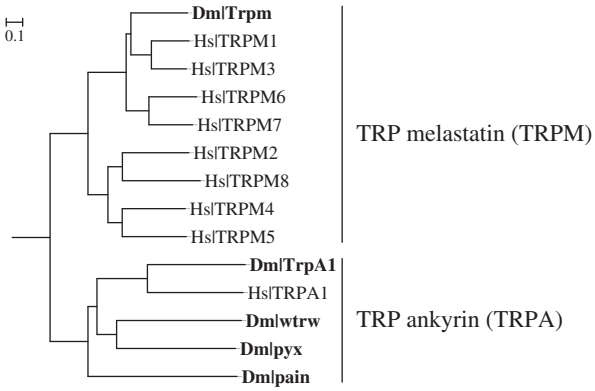

Figure 1. The *Drosophila melanogaster* (Dm) genome encodes one TRPM (Trpm) and four TRPA (TrpA1, painless, pyrexia, and water witch) channels. Mid-point rooted tree of *Drosophila* (Dm) and human (Hs) TRPMs and TRPAs.

2. Material and methods

(a) Animals

All *D. melanogaster* stocks were maintained at 24°C under a 12 : 12 light : dark cycle. In order to accelerate development, genetic crosses (and relevant controls) were raised for 5 days at 29°C under a 12 : 12 light : dark cycle. Wandering 3rd instar larvae were used for all experiments. The OregonR (ORR) strain was used to assess wild-type behaviour, and, where appropriate, the w^{1118} strain and outcrossed parental strains were used as genetic background controls. Transgenic and mutant strains included: $Trpm^{2}$ and $wtrw^{1}$ (gifts of K. Venkatachalam); $TrpA1^{W903*}$ and $TrpA1^{1}$ (gifts of W. D. Tracey); pyx^{3}, $pain^{70}$, and *Trpm* deficiency *Df(2R)XTE-11* (gifts of M. J. Galko); $GAL4^{GMR57C10}$ (pan-neuronal driver, BDSC no. 39171); $GAL4^{ppk}$ (CIV driver, BDSC no. 32079); *UAS-CaMPARI* (BDSC no. 58763); *UAS-TeTxLC* (active tetanus toxin, BDSC no. 28837); $UAS\text{-}IMP\text{-}TNT^{VI\text{-}A}$ (inactive tetanus toxin, BDSC no. 28840); *UAS-TrpA1-RNAi* 1 (BDSC no. 31384); *UAS-TrpA1-RNAi* 2 (BDSC no. 66905); *UAS-Trpm-RNAi* 1 (BDSC no. 31672); and *UAS-Trpm-RNAi* 2 (BDSC no. 31291).

(b) Behaviour

Crystalline L(-)-menthol (Acros Organics, Geel, Belgium) and icilin (Tocris Bioscience, Bristol, UK) were suspended in liquid dimethyl sulfoxide (DMSO) at various per cent weight/volume concentrations (% w/v): menthol (8%: 512 mM; 6%: 384 mM; 4%: 256 mM; 2%: 128 mM); icilin (0.5%: 16 mM; 1%: 32 mM; 15%: 482 mM). Solutions were discarded after 24 h. Individual larval subjects were placed in a well of a glass 9-well plate, and 10 µl of solution was delivered to the well via micropipette. Subjects were observed for 60 s and their behaviours recorded. In order to increase subject-background contrast in the representative images/videos, animals were left to freely locomote on a moist black arena, and menthol was applied as above.

(c) CaMPARI-based Ca^{2+} analyses

UAS-CaMPARI expression was driven via $GAL4^{GMR57C10}$. Live, freely behaving larvae were exposed to 8% menthol or vehicle

as described above. Photoconverting light was delivered under a Zeiss AxioZoom V16 microscope as previously described [50,51]. Larvae were subsequently placed in one drop of 1 : 5 diethyl ether : halocarbon oil and secured between a slide and slide cover. CIV neurons were imaged via a Zeiss LSM780 confocal microscope, and the resulting z-stacks were volume rendered as two-dimensional maximum intensity projections. Red and green fluorescence intensity was assessed using the FIJI distribution of ImageJ software.

(d) Electrophysiology

To record single-unit spiking activity of CIV neurons, we first prepared fillet preparations from *GAL4^{ppk}>UAS-mCD8::GFP* larvae. Larvae were placed in a Petri dish lined with Sylgard® 184 (Dow Corning, Midland, MI, USA) filled with HL-3 saline. The ventral body wall was cut open with fine scissors, and all muscles were carefully removed with a polished tungsten needle and scissors. The preparation was then constantly superfused with HL-3 saline at a rate of 1 ml min^{-1} at room temperature, and allowed to rest for more than 1 h before recording. Menthol was first dissolved in DMSO at a concentration of 500 mM and then diluted in HL-3 saline to a final concentration of 500 µM. Menthol was bath-applied to the specimen through superfusion. Extracellular recordings were made with a macropatch pipette (tip diameter, 5–10 µm) connected to the headstage of a patch-clamp amplifier (AxoPatch200B, Molecular Devices, Sunnyvale, CA, USA). Gentle suction was applied to draw the soma and a small portion of neurite into the pipette. The amplifier was set to the track mode to record neuronal spikes. The output signals from the amplifier were digitized at a sampling frequency of 10 kHz using a Micro1401 A/D converter (Cambridge Electronic Design, Cambridge, UK) and acquired into a laptop computer running Windows 10 with Spike2 software v. 8 (Cambridge Electric Design, Cambridge, UK). Average spike frequency was measured in a 30 s time window during baseline control conditions, superfusion of vehicle, and superfusion of menthol.

(e) Phylogenetics

Amino acid sequences for previously characterized TRP channels were collected from the following databases: JGI Genome (*Monosiga brevicollis*, *Nematostella vectensis* and *Daphnia pulex*), Ensembl (*Danio rerio*, *Gallus gallus* and *Strigamia maritima*), NCBI (*Hydra vulgaris*, *Homo sapiens*, *Mus musculus*, *Apis mellifera* and *Galendromus occidentalis*), WormBase (*Caenorhabditis elegans*) or FlyBase (*D. melanogaster*). *Panulirus argus* sequences were collected from [52]. In order to identify novel TRPM and TRPA channels, publically available protein models based on genomic and/or transcriptomic sequences for *Ac. digitifera* [53], *S. purpuratus* [54,55], *O. bimaculoides* [56], *P. caudatus* (BioProject PRJNA20497, GenBank AXZU00000000.2) and *Ap. californica* (BioProject, PRJNA209509, GenBank AASC00000000.3) were pBLASTed [57] against *D. melanogaster* TRP sequences. Sequences greater than 200 aa in length and with an *E*-value $< 1 \times 10^{-30}$ were retained and subsequently analysed via InterProScan [58]. Sequences which had predicted transmembrane segments and characteristic Ankyrin repeats (for TRPAs) were retained. Accession numbers are available in the electronic supplementary material, table S1.

Amino acid sequences were MUSCLE [59] aligned in MEGA7 [60]. Poorly aligned regions and spurious sequences were identified and trimmed using automated methods packaged with TrimAl [61]. As TRPA Ankyrin repeats were generally poorly aligned, they were manually removed prior to automated trimming by excluding everything N-terminal of 20 aa before the start of predicted transmembrane segment 1. IQ-Tree was then used to perform a composition chi-squared test in order to assess sequence homogeneity within TRP subfamilies [62]. Owing to extreme divergence, and in order to minimize possible topology disruptions owing to long branch attraction [63–65], *P. argus* TRPMm, TRPA-like1, and TRPA5-like1, and *C. elegans* TRPA-2 were excluded from final analyses; each failed the composition chi-squared test and introduced extremely long branches with weak support in a first-pass analysis. Final, trimmed alignments were used to generate phylogenetic trees. Bayesian trees were constructed in MrBayes (version 3.2.6) using a mixed amino acid substitution model and a gamma distributed rate of variation [66,67]. Two independent Markov chain Monte Carlo analyses (initial settings: 1 000 000 chains with sampling every 10) were run until convergence (less than 0.05). Twenty five per cent of the chain was considered burn-in and discarded. Maximum-likelihood trees were constructed in IQ-Tree using an amino acid substitution model automatically selected by ModelFinder [68]. Ultrafast bootstrapping (2000 bootstraps) was also performed in IQ-Tree [69]. Trees were visualized and edited in iTOL [70] and Adobe Illustrator CS6. Branches with low support (posterior probability less than 0.7 or bootstrap less than 70) were considered unresolved, and were collapsed to polytomies in the final trees. Ancestral sequence predictions were made in MEGA7 using the maximum-likelihood approach against previously generated alignments and Bayesian trees [71].

(f) Statistical analyses

Population proportions are presented as % ± standard error of the proportion (s.e.p.); differences in proportion were assessed using a generalized linear model with a logit link and a binomial error distribution, and pairwise comparisons were made using the lsmeans R package [72] and the Tukey method for multiple comparisons. CaMPARI photoconversion, spike frequency and latency measures are presented as mean ± standard error of the mean (s.e.m.); differences were assessed in GraphPad PRISM (GraphPad Software, La Jolla, California, USA) by unpaired *t*-test or ANOVA with Dunnett's *post hoc* test. Asterisk (*) indicates statistical significance $p < 0.05$, with significant *p*-values (as compared to wild-type or appropriate control) listed in the associated figure legend.

3. Results

(a) Menthol elicits *Trpm*- and *TrpA1*-dependent nocifensive rolling in *Drosophila* larvae

Vehicle (DMSO), menthol or icilin was topically applied to freely behaving *D. melanogaster* larvae, and their behaviour recorded (10 µl, delivered via micropipette). Mentholated solutions elicited a stereotyped rolling behaviour, identical to a previously described [73,74] nocifensive response (figure 2*a*; electronic supplementary material, movie S1). The proportion of animals which responded to menthol increased with higher menthol concentrations (figure 2*b*). By contrast, treatment with DMSO (figure 2*b*, vehicle; electronic supplementary material, movie S2) or icilin (figure 2*b*; electronic supplementary material, movie S3) did not elicit rolling.

Given TRP-dependent mechanisms of menthol sensing in vertebrates, we hypothesized that menthol-evoked rolling requires TRPM and TRPA channels. To test this, we assessed the behaviour of whole-animal *Trpm*, *TrpA1*, *pyx*, *pain*, and *wtrw* mutants. Compared to the control, a significantly smaller proportion of homozygous *TrpA1* and *Trpm* mutants rolled in response to menthol (figure 2*c*). Additionally, we observed a significantly increased latency to roll for those *TrpA1^{W903*}* mutants that did respond (figure 2*d*). By contrast, *pain*

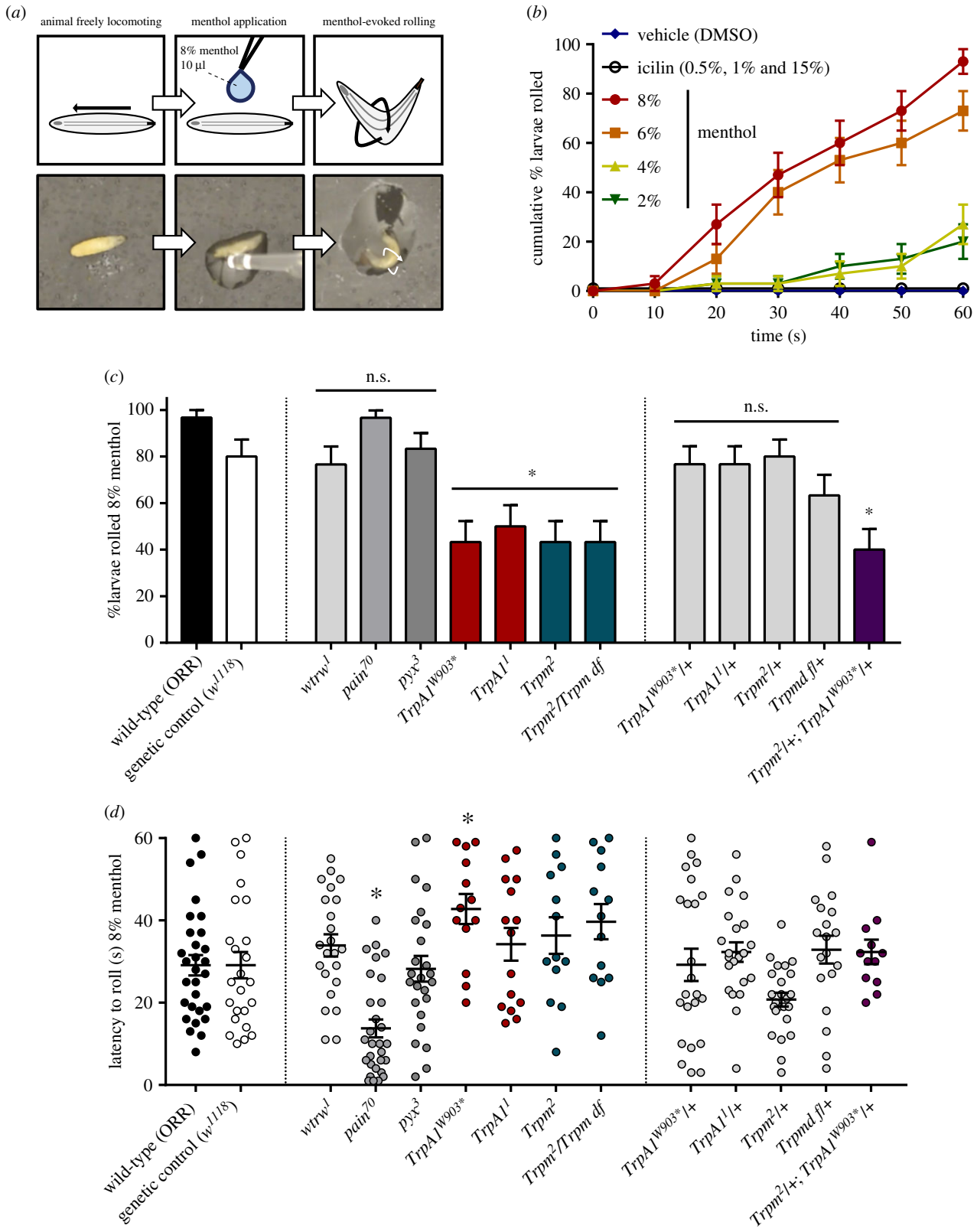

Figure 2. *Drosophila* larvae exhibit nocifensive rolling in response to menthol. (*a*) Menthol-evoked rolling. Top, cartoon. Bottom, video stills. (*b*) Cumulative proportion of wild-type rollers in response to menthol. The rolling response increased at higher menthol concentrations (% w/v). Cumulative proportion ± s.e.p. $n = 30$ for each condition. (*c*) Proportion of rollers in response to 8% menthol. Compared to wild-type, fewer *TrpA1* and *Trpm* mutants rolled in response to menthol ($TrpA1^{W903*}$, $p = 0.0221$; $TrpA1^{1}$, $p = 0.0479$; $Trpm^{2}$, $p = 0.0221$; $Trpm^{2}$/*Trpm df*, $p = 0.0221$). *Trpm* and *TrpA1* are haplosufficient for menthol sensitivity, but fewer transheterozygous mutants rolled in response to menthol ($p = 0.0090$). Proportions represented as % rollers ± s.e.p. $n = 30$ for each condition. (*d*) Latency to roll in response to 8% menthol. *painless* mutation sensitized rollers ($p = 0.0006$), while $TrpA1^{W903*}$ mutation desensitized rollers ($p = 0.0388$). Latency represented as time to roll in seconds ± s.e.m. *n* proportional to % rollers, where initial sample size was 30. (Online version in colour.)

mutation sensitized larvae to menthol—homozygous *pain* mutants rolled with severely decreased latency, and many rolled immediately following menthol application (figure 2*d*). Given that *painless* mutants could be sensitized to the point of immediately rolling following menthol application, it appears likely that menthol was rapidly delivered across the cuticle.

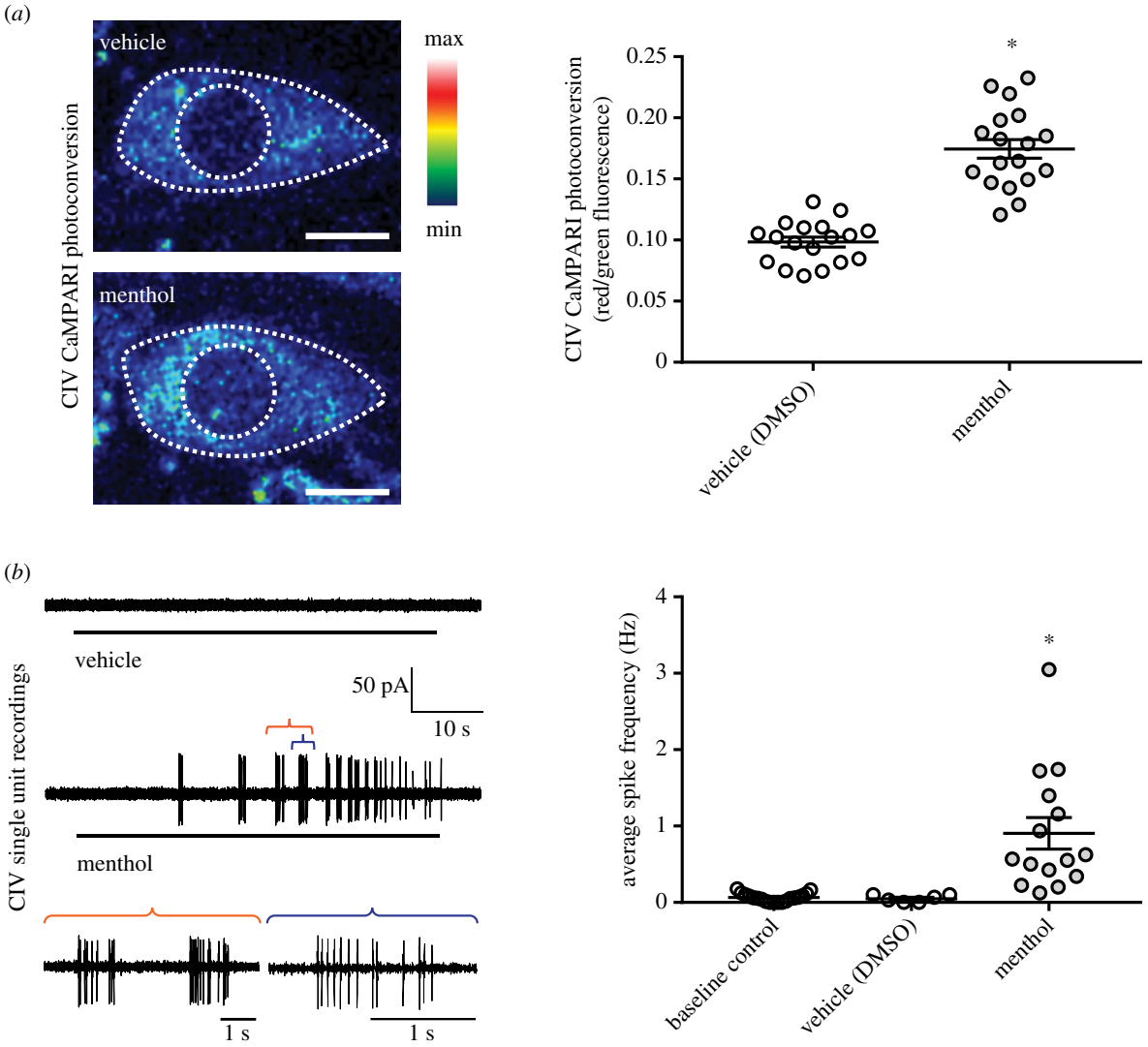

Figure 3. Menthol exposure activates Class IV (CIV) nociceptors. (*a*) Topical application of menthol to whole animals resulted in an increased CIV Ca^{2+} response relative to vehicle control. Left, representative CIV CaMPARI photoconversion visualized using a 16-colour lookup table. Right, CIV neurons were significantly activated by 8% menthol, as compared to vehicle control ($p < 0.0001$). Quantification of CaMPARI photoconversion by F_{red}/F_{green} CaMPARI fluorescence intensities. Photoconversion presented as mean ± s.e.m. $n = 18$ for each condition. (*b*) Bath application of menthol activated CIV neurons in filleted preparations relative to controls. Left, example CIV single-unit recordings (coloured brackets depict detailed view of strong menthol-evoked spiking activity). Right, menthol superfusion (500 µM) elicited significantly increased average spike frequency in CIV neurons ($p = 0.0001$). Average frequency in Hz ± s.e.m. Saline control, $n = 18$; DMSO control, $n = 6$; menthol, $n = 15$. (Online version in colour.)

As *TrpA1* and *Trpm* were both required for the menthol-evoked response, mutations were tested combinatorially. While heterozygous *TrpA1* (*TrpA1*^{W903*}/+ and *TrpA1*^{1}/+) and *Trpm* (*Trpm*^{2}/+ and *Trpm df*/+) mutants had no significant behavioural defects, transheterozygous (*TrpA1*^{W903*}/+; *Trpm*^{2}/+) mutants exhibited significantly inhibited menthol-evoked rolling, indicating that these channels genetically interact in menthol sensing (figure 2*c*).

(b) Class IV nociceptors mediate menthol-evoked rolling

Drosophila larvae have two known classes of peripheral nociceptors: multidendritic (md) Class III neurons are cold nociceptors and innocuous touch mechanosensors, whereas md CIV neurons are polymodal nociceptors which detect noxious heat, mechanical insults and short-wavelength light [33,34,74–78]. As rolling behaviour has been previously associated with CIV nociceptor activation, we hypothesized that menthol-evoked rolling requires CIV activation. In order to assess activation patterns *in vivo*, the *GAL4-UAS* system was used to drive neuronal expression of CaMPARI [79], a genetically encoded Ca^{2+} indicator. Live, freely behaving transgenic animals were exposed to menthol or vehicle, as above. The level of CIV neural activation was assessed *post hoc*, in live animals, as a green-to-red shift in CaMPARI fluorescence, which occurs in the presence of violet light as a function of increases in intracellular Ca^{2+} concentration. CaMPARI analyses revealed significant activation of CIV nociceptors in response to menthol, relative to vehicle control (figure 3*a*). To directly assess menthol-evoked activation of CIV neurons, we performed single-unit electrophysiological recordings of CIV neurons. Larvae were filleted, and mentholated saline solutions were superfused across the preparations. Electrophysiological recordings demonstrate that superfusion of menthol significantly increases spike frequency in CIV neurons relative to controls (figure 3*b*).

In order to test the necessity of CIV neurons for menthol-evoked rolling, genetically encoded active tetanus toxin (TNT) was used to block synaptic transmission in CIV neurons. GAL4^{ppk}-driven, CIV-specific expression of TNT completely ablated menthol-evoked rolling (figure 4).

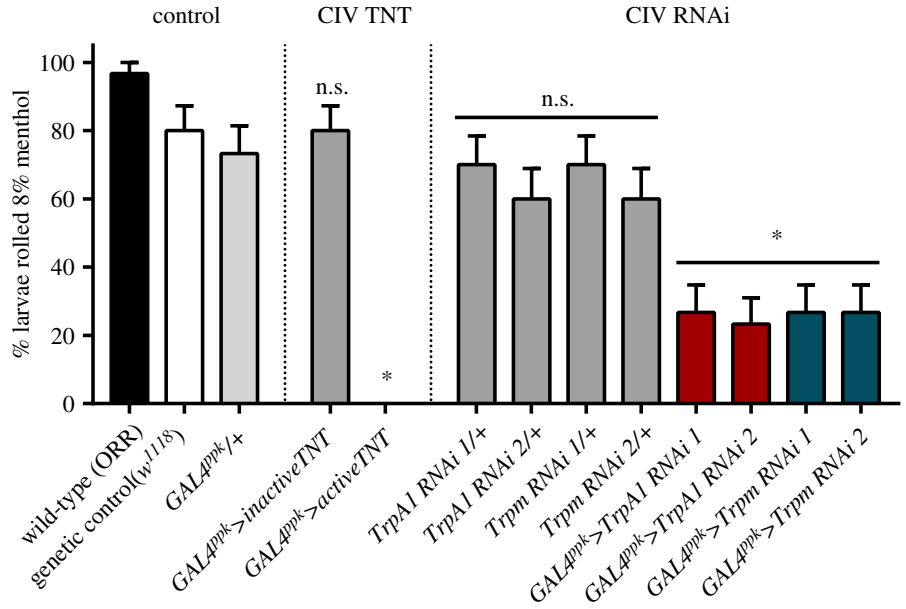

Figure 4. The TRP-dependent menthol response operates via CIV neurons. Silencing neural transmission in CIV neurons with active tetanus toxin (TNT) completely ablated the menthol response, while CIV-driven expression of inactive TNT did not significantly affect the rolling response. CIV-specific, RNAi-mediated knockdown using two independent transgenes for *TrpA1* and *Trpm* resulted in fewer animals rolling in response to menthol, as compared to the control (*TrpA1* RNAi 1, $p = 0.0032$; *TrpA1* RNAi *2*, $p = 0.0018$; *Trpm* RNAi 1, $p = 0.0032$; and *Trpm* RNAi 2, $p = 0.0032$). Proportions represented as % ± s.e.p. $n = 30$ for each condition. (Online version in colour.)

In light of TRP mutant and CIV TNT phenotypes, we hypothesized that menthol-evoked behaviour may be dependent on TrpA1 and/or Trpm function in CIV nociceptors. We previously demonstrated that *TrpA1* and *Trpm* transcripts are detectibly expressed in CIV nociceptors ([80], GEO: GSE46154). Consistent with these data, CIV-targeted, RNAi-mediated knockdown of *Trpm* or *TrpA1* strongly inhibited menthol-evoked rolling (figure 4), supporting a functional role for these TRP channels in CIV-mediated menthol sensing.

(c) Residues critical to menthol sensing were probably present in ancestral bilaterian channels

A number of specific amino acid residues have been associated with menthol sensitivity in mammalian TRPM [12,14,16,19,20] and TRPA [31] channels. Phylogenetic and sequence analyses were performed in order to assess how well conserved these residues are across taxa, and to infer their evolutionary history. The amino acid sequences for 69 TRPM channels and 56 TRPA channels (electronic supplementary material, table S1) were used to generate phylogenetic trees by both Bayesian and maximum-likelihood approaches. Trees were constructed using previously and newly characterized TRP sequences across a variety of metazoan species, with a choanoflagellate (*M. brevicollis*) outgroup (figure 5*a*). Both methods produced trees with largely consistent topologies (electronic supplementary material, figures S1–S4).

It has been previously noted that several species express TRPM-like channels which cluster independent of, or differ greatly from, other chordate and/or insect TRPMs [28,52,81]. In accordance with this, the consensus TRPM phylogeny shows a group of protostome TRPMs located basally, near choanoflagellate TRPMs (figure 5*b*, green). Previously published phylogenies have shown most arthropod TRPMs to be most closely related to chordate TRPMs 1, 3, 6 and 7, yet this relationship has not yet been formally discussed [25,28]. These trees demonstrate that non-basal TRPM channels group into two monophyletic clades (designated αTRPM and βTRPM), which collectively constitute all other analysed TRPM channels (figure 5*b*, red and blue). Each clade contains both protostome and deuterostome TRPMs and is rooted in cnidarian TRPMs, indicating that these two clades may have existed prior to the protostome–deuterostome split. The topology of these trees is consistent with a hypothesis that at least three distinct TRPM channels (designated basal TRPM, αTRPM and βTRPM) predate the last common bilaterian ancestor, Urbilateria. Further, this hypothesis is compatible with previously formulated hypotheses regarding the independent diversification of chordate TRPM channels [25,28,32].

As both α- and βTRPMs have been implicated in menthol sensing, ancestral sequence predictions were generated for ancestral bilaterian α- and βTRPM. Four TRPM8 residues—Y745, R842, Y1005 and L1009 (figure 5*d*, black arrows)—have been identified as critical to vertebrate menthol sensing [20]. Three of these residues, Y745, R842 and Y1005, are conserved in *Drosophila*, and ancestral sequence predictions suggest with high confidence that they are conserved from a common ancestral bilaterian sequence (figure 5*d*, bottom). The only site which differs from chordate TRPM8 is a predicted ancestral proline in place of L1009; proline, however, is more common at this site across TRPM channels, including in *Drosophila*, and previous work has shown that L1009P substitution in mouse TRPM8 does not affect menthol sensitivity [12].

For TRPAs, both previously characterized clades—TRPA1 and the 'basal' clade (figure 5*c*, orange and dark grey)—formed as expected, and conformed to other published topologies [7,27,28,32]. Although the term 'basal' has been used to describe other TRPAs, Peng *et al.* have suggested that the TRPA1 clade is the most ancestral [28]. This analysis does not clearly support nor undermine this hypothesis. What is clear, however, is that the TRPA1 clade predates the protostome–deuterostome split.

Previous work has shown that the TRPA1 pore region is important to mammalian menthol sensitivity. Serine and

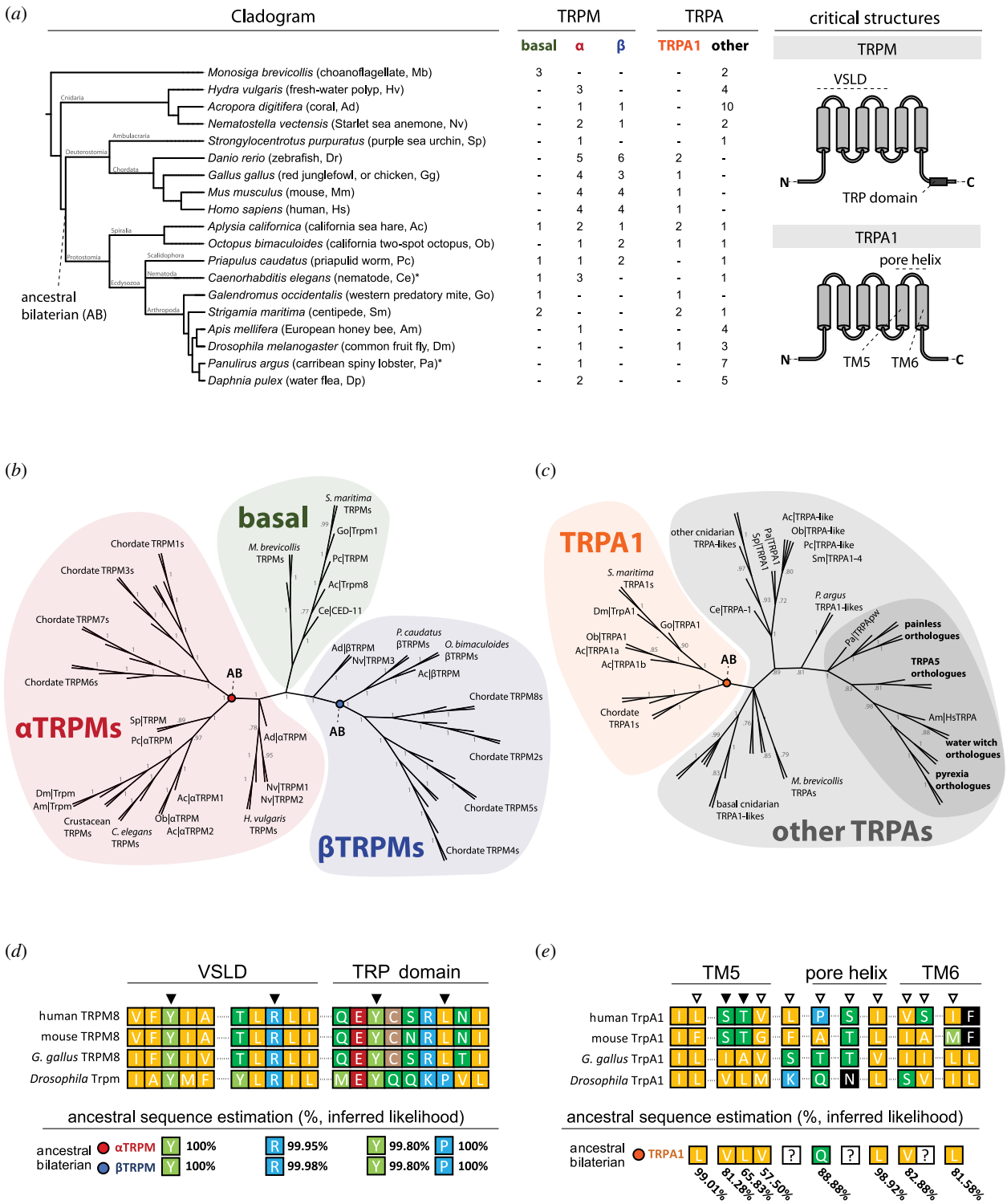

Figure 5. The evolutionary history of TRPM and TRPA channels, and of residues critical to menthol sensing. (*a*) Left, cladogram of species used in analysis. Asterisk (*) indicates that one or more previously known sequences were discarded owing to extreme divergence, as described in the Material and methods and electronic supplementary material. All sequence accession numbers are available in the electronic supplementary material. Right, domains previously identified as critical to menthol sensing. (*b*) Bayesian consensus tree for TRPM channels. Posterior probabilities are indicated for each internal branch. Branches with a posterior probability less than 0.70 were collapsed. For aesthetic purposes, branch lengths were ignored when generating this figure. Trees with branch lengths to scale are available in the electronic supplementary material. Green, basal clade; red, αTRPM clade; blue, βTRPM clade. (*c*) Bayesian consensus tree for TRPA channels, as in (*b*). Orange, TRPA1 clade; grey, other TRPAs; dark grey, clade previously described as 'basal'. (*d*) Alignment for select TRPM sequences and ancestral sequence estimations. Black arrows indicate previously identified critical residue site. % values represent probability of amino acid at the indicated site, at the colour-coded node. (*e*) Alignment for select TRPA sequences and ancestral sequence estimations, as in (*d*). White arrows indicate residues associated with species-specific menthol responses, in mammals. Question mark (?) indicates that no single amino acid was predicted with greater than 50% inferred likelihood.

threonine residues in TM5 are thought to be most critical to menthol sensitivity (figure 5*e*, black arrows), and a variety of others (figure 5*e*, white arrows) are associated with species-specific differences in menthol sensitivity [31]. These regions are generally poorly conserved between mammals and other species (figure 5*e*, top), including other chordates (e.g. *G. gallus*). In contrast to TRPM conservation, fewer critical TRPA1 residues appear to be consistently conserved from

a common bilaterian ancestor, and there is substantially less certainty as to the identity of these ancestral sequences (figure 5*e*, bottom).

4. Discussion

(a) Transient receptor potential-dependent transduction and menthol sensing in *Drosophila*

We have demonstrated that *Drosophila* larvae execute a dose-dependent, menthol-evoked, aversive rolling response consistent with the nocifensive behaviour displayed in response to noxious heat and mechanical insult. Cellularly, menthol exposure activates CIV nociceptors, and blocking synaptic transmission in these neurons inhibits menthol-evoked rolling. Molecularly, TrpA1 and Trpm are required for menthol-induced aversive behaviour, and genetically interact in this capacity.

Curiously, it has been previously reported that *Drosophila* TrpA1 does not directly gate in response to menthol [31]. The study in question, however, used lower concentrations of menthol applied to channels expressed *in vitro*. These sorts of discrepancies are not uncommon in studies of other TRPA1 modalities, and there are similar conflicting reports concerning TRPA1's role in cold nociception: some groups report that TRPA1 acts as a direct cold sensor, others state it responds to an indirect, cold-associated factor (reactive oxygen species and/or intracellular Ca^{2+}), while others claim it responds only to innocuous cooling, or does not respond to cold at all [47,82–86]; some isoforms of TRPA1 have been shown to directly gate in response to noxious high temperatures, yet high temperature nociception can be rescued by heat-insensitive isoforms [37]; and there is still debate as to whether or not TRPA1 functions similarly *in vivo* and *in vitro* [46]. Further, TRPA1s are differentially activated and/or inhibited by menthol, across species, across concentrations [41,47]. It is therefore unsurprising, if no less puzzling, that *Drosophila TrpA1* is required for menthol detection *in vivo*, yet the channel does not gate in response to relatively low concentrations of menthol *in vitro*. Instead, these and other findings suggest that we may not fully understand how TRPA1 functions, and that it may not be a simple sensor which directly responds to an incredibly wide variety of stimuli.

Moreover, although menthol and TRPA/TRPM interactions are most frequently studied, menthol is likely to be very promiscuous with respect to which channels it activates. Reports suggest that menthol activates, potentiates, or inhibits voltage-gated Na^{+} channels, L-type voltage-gated Ca^{2+} channels, the cystic fibrosis transmembrane conductance regulator, mouse TRPV3, TRPL, a wide variety of Ca^{2+}-dependent channels, as well as GABA, serotonin, and acetylcholine receptors [7,87–91]. Another notable player is the hymenopteran specific TRPA (HsTRPA), which is more closely related to Painless than to TRPA1 (figure 5*c*, dark grey). HsTRPA1 thermal sensitivity is depressed by application of menthol [7]. Given that *painless* mutants are hypersensitive to menthol (figure 2*c*), the so-called basal TRPAs may be complex mediators of chemo-sensitivity, rather than simple sensors. Currently, the menthol-specific ligand-binding and gating mechanisms of most receptors are not as well understood as those of chordate TRPA1 and TRPM8. However, these mechanisms are no doubt important, perhaps to species-specific behavioural responses, or to menthol's purported analgesic effect [2–4,88]. Future studies will need to investigate not only how other channels function in menthol sensing, but how they might interact with channels with incompletely understood activation properties (e.g. TRPA1), as these interactions may explain differences in menthol-evoked activity *in vivo* and *in vitro*.

(b) Transient receptor potential channels and the evolution of chemical nociception

Phylogenetic analyses have revealed that three TRPM clades—designated basal, αTRPM and βTRPM—and the TRPA1 clade, probably predate the protostome–deuterostome split. Further, many TRPM and TRPA1 residues critical to menthol sensing are conserved from ancestral bilaterian channels (although more variably so for TRPA1s). That residues critical to menthol sensing may predate the protostome–deuterostome split influences how we may understand the evolution of menthol production and avoidance. There is some evidence that menthol may be lethal to several insect species [10,11], including *D. melanogaster* [9]; as such, the ability to sense and respond to menthol may be adaptive. Given that there is considerable latency to roll in response to menthol (figure 2*d*), it is unclear if the aversive rolling behaviour is protective. Menthol sensing may be more important for adult females, which rather carefully select egg-laying sites and show aversion towards mentholated food [5]. Yet residues critical to menthol sensitivity substantially predate the emergence of Lamiaceae, the family of angiosperms that most notably produce menthol [92,93]. This appears consistent with early plants evolving menthol (or more broadly, terpene) production in order to repel animals, rather than early animal TRPs evolving menthol sensitivity in order to avoid certain plants. It is possible that animal TRP channels maintained menthol sensitivity since well before terrestrial animals encountered menthol producers, much like how mammalian TRP channels are sensitive to icilin, which is not known to be naturally occurring [1,16,84,94]. Pinpointing the exact origins of these abilities requires additional studies, in particular studies involving more basal (e.g. Xenacoelomorpha) and non-bilaterian species. Yet, it is conceivable that the functional capacity of these channels evolved in, or prior to, a common bilaterian ancestor, which inhabited a very different environment than extant terrestrial animals [95].

The structure of the urbilaterian nervous system is still under considerable debate [96–100]. However, given that TRP channels function in similar ways, in similar subsets of neurons, across taxa, it seems increasingly likely that ancestral TRP channels were expressed in some form of urbilaterian neural tissues, and that these tissues responded to external cues. Still, the function of conserved, menthol-associated residues in ancestral TRPs remains mysterious. However, while menthol production appears to be restricted to plants, terpene production (and more broadly, volatile organic compound production) is far more widespread. For example, volatile organic producers include plants, insects, protists, bacteria and fungi [101], which have been hypothesized to use volatile organic compounds in forms of microbial communication [102]. With this in mind, and concerning terpene sensing by early metazoan TRPs, one plausible hypothesis is that TRP-terpene sensitivity emerged as an early method of communication. Alternatively (or perhaps as sub-hypotheses), TRP-terpene sensing may have been employed as a mechanism by which to identify appropriate food sources, or to signal

potential danger, thereby avoiding damage from predation or infection—perhaps an early form of early nociception.

5. Conclusion

Herein, we have described cellular and molecular mechanisms by which *D. melanogaster* responds to menthol. Phylogenetic analyses revealed that extant TRPM channels are descended from three ancestral clades (basal, αTRPM and βTRPM), and that several residues critical to menthol sensing are conserved from common TRPM and TRPA1 ancestors. Collectively, these findings suggest that bilaterian menthol sensing has its origins in a common ancestor, and more broadly, contribute to a body of evidence suggesting that the mechanisms underlying TRP function and chemical nociception are ancient and highly conserved.

Data accessibility. Microarray data are available at NCBI Gene Expression Omnibus (accession number GSE46154; https://www.ncbi.nlm.nih.gov/geo/query/acc.cgi?acc=GSE46154). All other datasets supporting this article have been provided as part of the electronic supplementary material.

Authors' contributions. Conceptualization and experimental design, N.J.H., J.M.L., A.S. and D.N.C.; genetics, N.J.H. and J.M.L.; behaviour assays, N.J.H., J.M.L., M.N.B.; CaMPARI microscopy, N.J.H. and T.R.G.; electrophysiology, A.S.; phylogenetic and sequence analyses, N.J.H.; statistical analyses, N.J.H.; wrote the original manuscript, N.J.H.; critically analysed and edited the manuscript, N.J.H., J.M.L., A.S., T.R.G., M.N.B. and D.N.C.; approved the final draft, N.J.H., J.M.L., A.S., T.R.G., M.N.B. and D.N.C.; funding acquisition, N.J.H. and D.N.C.

Competing interests. We declare we have no competing interests.

Funding. This work was supported by the National Institute of Neurological Disorders and Stroke (NINDS) (R01NS086082; D.N.C.); the National Institute of General Medical Sciences (NIGMS) IMSD (R25GM109442-01A1; T.R.G. and D.N.C.); Georgia State University (GSU) Brains & Behavior Seed Grant (D.N.C.); GSU Brains & Behavior Fellowships (N.J.H. and J.M.L.); and the Kenneth W. and Georganne F. Honeycutt Fellowship (N.J.H.).

Acknowledgements. We would like to thank the Bloomington *Drosophila* Stock Center, as well as Drs Michael J. Galko, W. Dan Tracey and Kartik Venkatachalam for providing *Drosophila* strains.

References

1. Wei ET, Seid DA. 1983 AG-3–5: a chemical producing sensations of cold. *J. Pharm. Pharmacol.* **35**, 110–112. (doi:10.1111/j.2042-7158.1983.tb04279.x)
2. Romaneli RS, Boaratti AZ, Rodrigues AT, Queiroz MA, Khan KU, Nascimento TMT, Fernandes JBK, Mansano CFM. 2018 Efficacy of benzocaine, eugenol and menthol as anesthetics for freshwater angelfish (*Pterophyllum scalare*). *J. Aquat. Anim. Health* **30**, 210–216. (doi:10.1002/aah.10030)
3. Liu B, Jordt S-E. 2018 Cooling the itch via TRPM8. *J. Invest. Dermatol.* **138**, 1254–1256. (doi:10.1016/j.jid.2018.01.020)
4. Ton HT, Phan TX, Abramyan AM, Shi L, Ahern GP. 2017 Identification of a putative binding site critical for general anesthetic activation of TRPA1. *Proc. Natl Acad. Sci. USA* **114**, 3762–3767. (doi:10.1073/pnas.1618144114)
5. Abed-Vieillard D, Cortot J. 2016 When choice makes sense: menthol influence on mating, oviposition and fecundity in *Drosophila melanogaster*. *Front. Integr. Neurosci.* **10**, 5. (doi:10.3389/fnint.2016.00005)
6. Abed-Vieillard D, Cortot J, Everaerts C, Ferveur J-F. 2014 Choice alters *Drosophila* oviposition site preference on menthol. *Biol. Open* **3**, 22–28. (doi:10.1242/bio.20136973)
7. Kohno K, Sokabe T, Tominaga M, Kadowaki T. 2010 Honey bee thermal/chemical sensor, AmHsTRPA, reveals neofunctionalization and loss of transient receptor potential channel genes. *J. Neurosci.* **30**, 12 219–12 229. (doi:10.1523/JNEUROSCI.2001-10.2010)
8. Maliszewska J, Jankowska M, Kletkiewicz H, Stankiewicz M, Rogalska J. 2018 Effect of capsaicin and other thermo-TRP agonists on thermoregulatory processes in the American cockroach. *Molecules* **23**, 3360. (doi:10.3390/molecules23123360).
9. Thorpe WH. 1939 Further studies on pre-imaginal olfactory conditioning in insects. *Proc. R. Soc. Lond. B* **127**, 424–433. (doi:10.1098/rspb.1939.0032)
10. Rice PJ, Coats J. 1994 Insecticidal properties of several monoterpenoids to the house fly (Diptera: Muscidae), red flour beetle (Coleoptera: Tenebrionidae), and southern corn rootworm (Coleoptera: Chrysomelidae). *J. Econ. Entomol.* **87**, 1172–1179. (doi:10.1093/jee/87.5.1172)
11. Samarasekera R, Weerasinghe Indira S, Hemalal KDP. 2007 Insecticidal activity of menthol derivatives against mosquitoes. *Pest Manag. Sci.* **64**, 290–295. (doi:10.1002/ps.1516)
12. Bandell M, Dubin AE, Petrus MJ, Orth A, Mathur J, Hwang SW, Patapoutian A. 2006 High-throughput random mutagenesis screen reveals TRPM8 residues specifically required for activation by menthol. *Nat. Neurosci.* **9**, 493–500. (doi:10.1038/nn1665)
13. Janssens A, Voets T. 2011 Ligand stoichiometry of the cold- and menthol-activated channel TRPM8. *J. Physiol.* **589**, 4827–4835. (doi:10.1113/jphysiol.2011.216523)
14. Malkia A, Pertusa M, Fernández-Ballester G, Ferrer-Montiel A, Viana F. 2009 Differential role of the menthol-binding residue Y745 in the antagonism of thermally gated TRPM8 channels. *Mol. Pain* **5**, 1744–8069. (doi:10.1186/1744-8069-5-62)
15. Myers BR, Sigal YM, Julius D. 2009 Evolution of thermal response properties in a cold-activated TRP channel. *PLoS ONE* **4**, e5741. (doi:10.1371/journal.pone.0005741)
16. Pedretti A, Marconi C, Bettinelli I, Vistoli G. 2009 Comparative modeling of the quaternary structure for the human TRPM8 channel and analysis of its binding features. *Biochim. Biophys. Acta Biomembr.* **1788**, 973–982. (doi:10.1016/j.bbamem.2009.02.007)
17. Peier AM *et al.* 2002 A TRP channel that senses cold stimuli and menthol. *Cell* **108**, 705–715. (doi:10.1016/S0092-8674(02)00652-9)
18. Pertusa M, Rivera B, González A, Ugarte G, Madrid R. 2018 Critical role of the pore domain in the cold response of TRPM8 channels identified by ortholog functional comparison. *J. Biol. Chem.* **293**, 12 454–12 471. (doi:10.1074/jbc.RA118.002256)
19. Rath P, Hilton JK, Sisco NJ, Van Horn WD. 2016 Implications of human transient receptor potential melastatin 8 (TRPM8) channel gating from menthol binding studies of the sensing domain. *Biochemistry* **55**, 114–124. (doi:10.1021/acs.biochem.5b00931)
20. Yin Y, Wu M, Zubcevic L, Borschel WF, Lander GC, Lee S-Y. 2018 Structure of the cold- and menthol-sensing ion channel TRPM8. *Science* **359**, 237–241. (doi:10.1126/science.aan4325)
21. Karashima Y, Damann N, Prenen J, Talavera K, Segal A, Voets T, Nilius B. 2007 Bimodal action of menthol on the transient receptor potential channel TRPA1. *J. Neurosci.* **27**, 9874. (doi:10.1523/jneurosci.2221-07.2007)
22. McKemy DD, Neuhausser WM, Julius D. 2002 Identification of a cold receptor reveals a general role for TRP channels in thermosensation. *Nature* **416**, 52–58. (doi:10.1038/nature719)
23. Macpherson LJ, Dubin AE, Evans MJ, Marr F, Schultz PG, Cravatt BF, Patapoutian A. 2007 Noxious compounds activate TRPA1 ion channels through covalent modification of cysteines. *Nature* **445**, 541–545. (doi:10.1038/nature05544)
24. Story GM *et al.* 2003 ANKTM1, a TRP-like channel expressed in nociceptive neurons, is activated by cold temperatures. *Cell* **112**, 819–829. (doi:10.1016/S0092-8674(03)00158-2)
25. Saito S, Shingai R. 2006 Evolution of thermoTRP ion channel homologs in vertebrates. *Physiol.*

Genomics **27**, 219–230. (doi:10.1152/physiolgenomics.00322.2005)

26. Dhaka A, Murray AN, Mathur J, Earley TJ, Petrus MJ, Patapoutian A. 2007 TRPM8 is required for cold sensation in mice. *Neuron* **54**, 371–378. (doi:10.1016/j.neuron.2007.02.024)
27. Kang K, Pulver SR, Panzano VC, Chang EC, Griffith LC, Theobald DL, Garrity PA. 2010 Analysis of *Drosophila* TRPA1 reveals an ancient origin for human chemical nociception. *Nature* **464**, 597–600. (doi:10.1038/nature08848)
28. Peng G, Shi X, Kadowaki T. 2015 Evolution of TRP channels inferred by their classification in diverse animal species. *Mol. Phylogenet. Evol.* **84**, 145–157. (doi:10.1016/j.ympev.2014.06.016)
29. Jordt S-E, Bautista DM, Chuang H-H, McKemy DD, Zygmunt PM, Högestätt ED, Meng ID, Julius D. 2004 Mustard oils and cannabinoids excite sensory nerve fibres through the TRP channel ANKTM1. *Nature* **427**, 260–265. (doi:10.1038/nature02282)
30. Vandewauw I *et al.* 2018 A TRP channel trio mediates acute noxious heat sensing. *Nature* **555**, 662–666. (doi:10.1038/nature26137)
31. Xiao B, Dubin AE, Bursulaya B, Viswanath V, Jegla TJ, Patapoutian A. 2008 Identification of the transmembrane domain five as a critical molecular determinant of menthol sensitivity in mammalian TRPA1 channels. *J. Neurosci.* **28**, 9640–9651. (doi:10.1523/JNEUROSCI.2772-08.2008)
32. Matsuura H, Sokabe T, Kohno K, Tominaga M, Kadowaki T. 2009 Evolutionary conservation and changes in insect TRP channels. *BMC Evol. Biol.* **9**, 228. (doi:10.1186/1471-2148-9-228)
33. Turner HN *et al.* 2016 The TRP channels Pkd2, NompC, and Trpm act in cold-sensing neurons to mediate unique aversive behaviors to noxious cold in *Drosophila*. *Curr. Biol.* **26**, 3116–3128. (doi:10.1016/j.cub.2016.09.038)
34. Himmel NJ, Patel AA, Cox DN. 2017 Invertebrate nociception. In *The Oxford research encyclopedia of neuroscience* (ed. PS Katz). Oxford, UK: Oxford University Press. (doi:10.1093/acrefore/9780190264086.013.166)
35. Kim SH, Lee Y, Akitake B, Woodward OM, Guggino WB, Montell C. 2010 *Drosophila* TRPA1 channel mediates chemical avoidance in gustatory receptor neurons. *Proc. Natl Acad. Sci. USA* **107**, 8440. (doi:10.1073/pnas.1001425107)
36. Neely GG *et al.* 2011 TrpA1 regulates thermal nociception in *Drosophila*. *PLoS ONE* **6**, e24343. (doi:10.1371/journal.pone.0024343)
37. Zhong L, Bellemer A, Yan H, Honjo K, Robertson J, Hwang RY, Pitt GS, Tracey WD. 2012 Thermosensory and nonthermosensory isoforms of *Drosophila melanogaster* TRPA1 reveal heat-sensor domains of a ThermoTRP channel. *Cell Rep.* **1**, 43–55. (doi:10.1016/j.celrep.2011.11.002)
38. Peng G, Kashio M, Li T, Dong X, Tominaga M, Kadowaki T. 2016 TRPA1 channels in *Drosophila* and honey bee ectoparasitic mites share heat sensitivity and temperature-related physiological functions. *Front. Physiol.* **7**, 447. (doi:10.3389/fphys.2016.00447)
39. Wang X, Li T, Kashio M, Xu Y, Tominaga M, Kadowaki T. 2018 HsTRPA of the red imported fire ant, *Solenopsis invicta*, functions as a nocisensor and uncovers the evolutionary plasticity of HsTRPA channels. *eNeuro* **5**, ENEURO.0327-0317.2018. (doi:10.1523/ENEURO.0327-17.2018)
40. Gracheva EO *et al.* 2010 Molecular basis of infrared detection by snakes. *Nature* **464**, 1006–1011. (doi:10.1038/nature08943)
41. Moparthi L *et al.* 2016 Human TRPA1 is a heat sensor displaying intrinsic U-shaped thermosensitivity. *Sci. Rep.* **6**, 28763. (doi:10.1038/srep28763)
42. Saito CT, Fukuta N, Tominaga M, Saito S, Ohta T, Takahashi K, Banzawa N, Imagawa T 2014 Heat and noxious chemical sensor, chicken TRPA1, as a target of bird repellents and identification of its structural determinants by multispecies functional comparison. *Mol. Biol. Evol.* **31**, 708-–722. (doi:10.1093/molbev/msu001)
43. Saito S, Nakatsuka K, Takahashi K, Fukuta N, Imagawa T, Ohta T, Tominaga M. 2012 Analysis of transient receptor potential ankyrin 1 (TRPA1) in frogs and lizards illuminates both nociceptive heat and chemical sensitivities and coexpression with TRP vanilloid 1 (TRPV1) in ancestral vertebrates. *J. Biol. Chem.* **287**, 30 743–30 754. (doi:10.1074/jbc.M112.362194)
44. Sato A, Sokabe T, Kashio M, Yasukochi Y, Tominaga M, Shiomi K. 2014 Embryonic thermosensitive TRPA1 determines transgenerational diapause phenotype of the silkworm, *Bombyx mori*. *Proc. Natl Acad. Sci. USA* **111**, E1249–E1255. (doi:10.1073/pnas.1322134111)
45. Wang G, Qiu YT, Lu T, Kwon H-W, Pitts RJ, Van Loon JJA, Takken W, Zwiebel LJ. 2009 *Anopheles gambiae* TRPA1 is a heat-activated channel expressed in thermosensitive sensilla of female antennae. *Eur. J. Neurosci.* **30**, 967–974. (doi:10.1111/j.1460-9568.2009.06901.x)
46. Caspani O, Heppenstall PA. 2009 TRPA1 and cold transduction: an unresolved issue? *J. Gen. Physiol.* **133**, 245–249. (doi:10.1085/jgp.200810136)
47. Chen J, Kang D, Xu J, Lake M, Hogan JO, Sun C, Walter K, Yao B, Kim D. 2013 Species differences and molecular determinant of TRPA1 cold sensitivity. *Nat. Commun.* **4**, 2501. (doi:10.1038/ncomms3501)
48. Saito S, Tominaga M. 2017 Evolutionary tuning of TRPA1 and TRPV1 thermal and chemical sensitivity in vertebrates. *Temperature (Austin)* **4**, 141–152. (doi:10.1080/23328940.2017.1315478)
49. Walters ET. 2018 Nociceptive biology of molluscs and arthropods: evolutionary clues about functions and mechanisms potentially related to pain. *Front. Physiol.* **9**, 1049. (doi:10.3389/fphys.2018.01049)
50. Im SH, Patel AA, Cox DN, Galko MJ. 2018 *Drosophila* insulin receptor regulates the persistence of injury-induced nociceptive sensitization. *Dis. Model. Mech.* **11**, dmm034231. (doi:10.1242/dmm.034231)
51. Patel AA, Cox DN. 2017 Behavioral and functional assays for investigating mechanisms of noxious cold detection and multimodal sensory processing in *Drosophila* larvae. *Bio Protoc.* **7**, e2388. (doi:10.21769/BioProtoc.2388)
52. Kozma MT, Schmidt M, Ngo-Vu H, Sparks SD, Senatore A, Derby CD. 2018 Chemoreceptor proteins in the Caribbean spiny lobster, *Panulirus argus*: expression of ionotropic receptors, gustatory receptors, and TRP channels in two chemosensory organs and brain. *PLoS ONE* **13**, e0203935. (doi:10.1371/journal.pone.0203935)
53. Shinzato C *et al.* 2011 Using the *Acropora digitifera* genome to understand coral responses to environmental change. *Nature* **476**, 320. (doi:10.1038/nature10249)
54. Kudtarkar P, Cameron RA. 2017 Echinobase: an expanding resource for echinoderm genomic information. *Database* **2017**, bax074. (doi:10.1093/database/bax074)
55. Yuan A, He D, Davidson E, Samanta M, Cameron RA. 2008 SpBase: the sea urchin genome database and web site. *Nucleic Acids Res.* **37**, D750–D754. (doi:10.1093/nar/gkn887)
56. Albertin CB, Simakov O, Mitros T, Wang ZY, Pungor JR, Edsinger-Gonzales E, Brenner S, Ragsdale CW, Rokhsar DS. 2015 The octopus genome and the evolution of cephalopod neural and morphological novelties. *Nature* **524**, 220–224. (doi:10.1038/nature14668)
57. Altschul SF, Madden TL, Schäffer AA, Zhang J, Zhang Z, Miller W, Lipman DJ. 1997 Gapped BLAST and PSI-BLAST: a new generation of protein database search programs. *Nucleic Acids Res.* **25**, 3389–3402. (doi:10.1093/nar/25.17.3389)
58. Jones P *et al.* 2014 InterProScan 5: genome-scale protein function classification. *Bioinformatics* **30**, 1236–1240. (doi:10.1093/bioinformatics/btu031)
59. Edgar RC. 2004 MUSCLE: multiple sequence alignment with high accuracy and high throughput. *Nucleic Acids Res.* **32**, 1792–1797. (doi:10.1093/nar/gkh340)
60. Stecher G, Kumar S, Tamura K. 2016 MEGA7: molecular evolutionary genetics analysis version 7.0 for bigger datasets. *Mol. Biol. Evol.* **33**, 1870–1874. (doi:10.1093/molbev/msw054)
61. Capella-Gutiérrez S, Silla-Martínez JM, Gabaldón T. 2009 trimAl: a tool for automated alignment trimming in large-scale phylogenetic analyses. *Bioinformatics* **25**, 1972–1973. (doi:10.1093/bioinformatics/btp348)
62. Schmidt HA, Minh BQ, von Haeseler A, Nguyen L-T. 2014 IQ-TREE: a fast and effective stochastic algorithm for estimating maximum-likelihood phylogenies. *Mol. Biol. Evol.* **32**, 268–274. (doi:10.1093/molbev/msu300)
63. Goldman N, Parks SL. 2014 Maximum likelihood inference of small trees in the presence of long branches. *Syst. Biol.* **63**, 798–811. (doi:10.1093/sysbio/syu044)
64. Kück P, Mayer C, Wägele J-W, Misof B. 2012 Long branch effects distort maximum likelihood phylogenies in simulations despite selection of the

correct model. *PLoS ONE* **7**, e36593. (doi:10.1371/journal.pone.0036593)

65. Philippe H, Zhou Y, Brinkmann H, Rodrigue N, Delsuc F. 2005 Heterotachy and long-branch attraction in phylogenetics. *BMC Evol. Biol.* **5**, 50. (doi:10.1186/1471-2148-5-50)
66. Huelsenbeck JP, Ronquist F, Nielsen R, Bollback JP. 2001 Bayesian inference of phylogeny and its impact on evolutionary biology. *Science* **294**, 2310–2314. (doi:10.1126/science.1065889)
67. Ronquist F, Huelsenbeck JP. 2003 MrBayes 3: Bayesian phylogenetic inference under mixed models. *Bioinformatics* **19**, 1572–1574. (doi:10.1093/bioinformatics/btg180)
68. Kalyaanamoorthy S, Minh BQ, Wong TKF, von Haeseler A, Jermiin LS. 2017 ModelFinder: fast model selection for accurate phylogenetic estimates. *Nat. Methods* **14**, 587–589. (doi:10.1038/nmeth.4285)
69. Hoang DT, Vinh LS, Chernomor O, Minh BQ, von Haeseler A. 2017 UFBoot2: improving the ultrafast bootstrap approximation. *Mol. Biol. Evol.* **35**, 518–522. (doi:10.1093/molbev/msx281)
70. Letunic I, Bork P. 2016 Interactive tree of life (iTOL) v3: an online tool for the display and annotation of phylogenetic and other trees. *Nucleic Acids Res.* **44**, W242–W245. (doi:10.1093/nar/gkw290)
71. Thornton JM, Jones DT, Taylor WR. 1992 The rapid generation of mutation data matrices from protein sequences. *Bioinformatics* **8**, 275–282. (doi:10.1093/bioinformatics/8.3.275)
72. Lenth RV. 2016 Least-squares means: the R package lsmeans. *J. Stat. Softw.* **69**, 33. (doi:10.18637/jss.v069.i01)
73. Hwang RY, Zhong L, Xu Y, Johnson T, Zhang F, Deisseroth K, Tracey WD. 2007 Nociceptive neurons protect *Drosophila* larvae from parasitoid wasps. *Curr. Biol.* **17**, 2105–2116. (doi:10.1016/j.cub.2007.11.029)
74. Tracey WD, Wilson RI, Laurent G, Benzer S. 2003 *painless*, a *Drosophila* gene essential for nociception. *Cell* **113**, 261–273. (doi:10.1016/S0092-8674(03)00272-1)
75. Im SH, Galko MJ. 2012 Pokes, sunburn, and hot sauce: *Drosophila* as an emerging model for the biology of nociception. *Dev. Dyn.* **241**, 16–26. (doi:10.1002/dvdy.22737)
76. Tsubouchi A, Caldwell JC, Tracey WD. 2012 Dendritic filopodia, Ripped Pocket, NOMPC, and NMDARs contribute to the sense of touch in *Drosophila* larvae. *Curr. Biol.* **22**, 2124–2134. (doi:10.1016/j.cub.2012.09.019)
77. Xiang Y, Yuan Q, Vogt N, Looger LL, Jan LY, Jan YN. 2010 Light-avoidance-mediating photoreceptors tile the *Drosophila* larval body wall. *Nature* **468**, 921–926. (doi:10.1038/nature09576)
78. Yan Z, Zhang W, He Y, Gorczyca D, Xiang Y, Cheng LE, Meltzer S, Jan LY, Jan YN. 2013 *Drosophila* NOMPC is a mechanotransduction channel subunit for gentle-touch sensation. *Nature* **493**, 221–225. (doi:10.1038/nature11685)
79. Fosque BF *et al.* 2015 Labeling of active neural circuits *in vivo* with designed calcium integrators. *Science* **347**, 755–760. (doi:10.1126/science.1260922)
80. Iyer EPR, Iyer SC, Sullivan L, Wang D, Meduri R, Graybeal LL, Cox DN. 2013 Functional genomic analyses of two morphologically distinct classes of *Drosophila* sensory neurons: post-mitotic roles of transcription factors in dendritic patterning. *PLoS ONE* **8**, e72434. (doi:10.1371/journal.pone.0072434)
81. Driscoll K, Stanfield GM, Droste R, Horvitz HR. 2017 Presumptive TRP channel CED-11 promotes cell volume decrease and facilitates degradation of apoptotic cells in *Caenorhabditis elegans*. *Proc. Natl Acad. Sci. USA* **114**, 8806–8811. (doi:10.1073/pnas.1705084114)
82. Arenas OM, Zaharieva EE, Para A, Vásquez-Doorman C, Petersen CP, Gallio M. 2017 Activation of planarian TRPA1 by reactive oxygen species reveals a conserved mechanism for animal nociception. *Nat. Neurosci.* **20**, 1686–1693. (doi:10.1038/s41593-017-0005-0)
83. Chatzigeorgiou M *et al.* 2010 Specific roles for DEG/ENaC and TRP channels in touch and thermosensation in *C. elegans* nociceptors. *Nat. Neurosci.* **13**, 861–868. (doi:10.1038/nn.2581)
84. Doerner JF, Gisselmann G, Hatt H, Wetzel CH. 2007 Transient receptor potential channel A1 is directly gated by calcium ions. *J. Biol. Chem.* **282**, 13 180–13 189. (doi:10.1074/jbc.M607849200)
85. Sawada Y, Hosokawa H, Hori A, Matsumura K, Kobayashi S. 2007 Cold sensitivity of recombinant TRPA1 channels. *Brain Res.* **1160**, 39–46. (doi:10.1016/j.brainres.2007.05.047)
86. Zurborg S, Yurgionas B, Jira JA, Caspani O, Heppenstall PA. 2007 Direct activation of the ion channel TRPA1 by Ca^{2+}. *Nat. Neurosci.* **10**, 277–279. (doi:10.1038/nn1843)
87. Gaudioso C, Hao J, Martin-Eauclaire M-F, Gabriac M, Delmas P. 2012 Menthol pain relief through cumulative inactivation of voltage-gated sodium channels. *Pain* **153**, 473–484. (doi:10.1016/j.pain.2011.11.014)
88. Macpherson LJ, Hwang SW, Miyamoto T, Dubin AE, Patapoutian A, Story GM. 2006 More than cool: promiscuous relationships of menthol and other sensory compounds. *Mol. Cell. Neurosci.* **32**, 335–343. (doi:10.1016/j.mcn.2006.05.005)
89. Morise M *et al.* 2010 Heterologous regulation of anion transporters by menthol in human airway epithelial cells. *Eur. J. Pharmacol.* **635**, 204–211. (doi:10.1016/j.ejphar.2010.03.032)
90. Oz M, El Nebrisi EG, Yang K-HS, Howarth FC, Al Kury LT. 2017 Cellular and molecular targets of menthol actions. *Front. Pharmacol.* **8**, 472. (doi:10.3389/fphar.2017.00472)
91. Parnas M, Peters M, Dadon D, Lev S, Vertkin I, Slutsky I, Minke B. 2009 Carvacrol is a novel inhibitor of *Drosophila* TRPL and mammalian TRPM7 channels. *Cell Calcium* **45**, 300–309. (doi:10.1016/j.ceca.2008.11.009)
92. Drew BT, Sytsma KJ. 2012 Phylogenetics, biogeography, and staminal evolution in the tribe Mentheae (Lamiaceae). *Am. J. Bot.* **99**, 933–953. (doi:10.3732/ajb.1100549)
93. Singh B, Sharma RA. 2015 Plant terpenes: defense responses, phylogenetic analysis, regulation and clinical applications. *3 Biotech* **5**, 129–151. (doi:10.1007/s13205-014-0220-2)
94. Kühn FJP, Witschas K, Kühn C, Lückhoff A. 2010 Contribution of the S5-pore-S6 domain to the gating characteristics of the cation channels TRPM2 and TRPM8. *J. Biol. Chem.* **285**, 26 806–26 814. (doi:10.1074/jbc.M110.109975)
95. Valentine JW. 2002 Prelude to the Cambrian explosion. *Annu. Rev. Earth Planet Sci.* **30**, 285–306. (doi:10.1146/annurev.earth.30.082901.092917)
96. Bailly X, Reichert H, Hartenstein V. 2013 The urbilaterian brain revisited: novel insights into old questions from new flatworm clades. *Dev. Genes Evol.* **223**, 149–157. (doi:10.1007/s00427-012-0423-7)
97. Hejnol A, Martindale MQ. 2008 Acoel development supports a simple planula-like urbilaterian. *Phil. Trans. R. Soc. B* **363**, 1493–1501. (doi:10.1098/rstb.2007.2239)
98. Moroz LL. 2009 On the independent origins of complex brains and neurons. *Brain Behav. Evol.* **74**, 177–190. (doi:10.1159/000258665)
99. Moroz LL. 2012 Phylogenomics meets neuroscience: how many times might complex brains have evolved? *Acta Biol. Hung.* **63**(Suppl 2), 3–19. (doi:10.1556/ABiol.63.2012.Suppl.2.1)
100. Northcutt RG. 2010 Cladistic analysis reveals brainless urbilateria. *Brain Behav. Evol.* **76**, 1–2. (doi:10.1159/000316443)
101. Schulz-Bohm K, Martín-Sánchez L, Garbeva P. 2017 Microbial volatiles: small molecules with an important role in intra- and inter-kingdom interactions. *Front. Microbiol.* **8**, 2484. (doi:10.3389/fmicb.2017.02484)
102. Schmidt R *et al.* 2017 Fungal volatile compounds induce production of the secondary metabolite Sodorifen in *Serratia plymuthica* PRI-2C. *Sci. Rep.* **7**, 862. (doi:10.1038/s41598-017-00893-3)